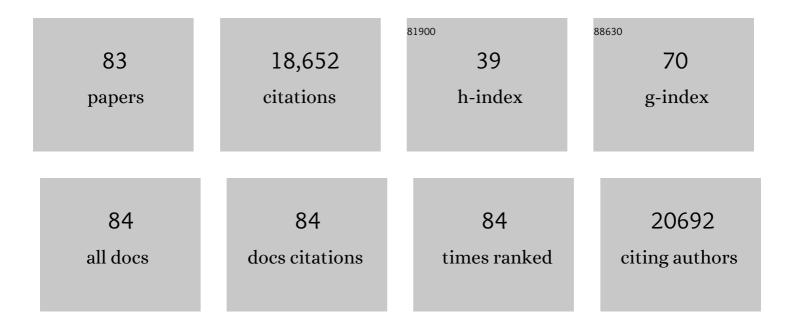
List of Publications by Year in descending order

Source: https://exaly.com/author-pdf/7925084/publications.pdf Version: 2024-02-01



CEEDT IS LITIENS

| # | Article | IF | CITATIONS |
|----|---|------|-----------|
| 1 | Streaming Convolutional Neural Networks for End-to-End Learning With Multi-Megapixel Images. IEEE Transactions on Pattern Analysis and Machine Intelligence, 2022, 44, 1581-1590. | 13.9 | 28 |
| 2 | Using deep learning for quantification of cellularity and cell lineages in bone marrow biopsies and comparison to normal age-related variation. Pathology, 2022, 54, 318-327. | 0.6 | 6 |
| 3 | Artificial intelligence for diagnosis and Gleason grading of prostate cancer: the PANDA challenge. Nature Medicine, 2022, 28, 154-163. | 30.7 | 143 |
| 4 | Automated quantification of levels of breast terminal duct lobular (TDLU) involution using deep learning. Npj Breast Cancer, 2022, 8, 13. | 5.2 | 6 |
| 5 | Automatic tumour segmentation in H&E-stained whole-slide images of the pancreas , 2022, , . | | 0 |
| 6 | A Decade of <i>GigaScience</i> : The Challenges of Gigapixel Pathology Images. GigaScience, 2022, 11, . | 6.4 | 3 |
| 7 | Predicting biochemical recurrence of prostate cancer with artificial intelligence. Communications Medicine, 2022, 2, . | 4.2 | 8 |
| 8 | The Medical Segmentation Decathlon. Nature Communications, 2022, 13, . | 12.8 | 252 |
| 9 | Prostate158 - An expert-annotated 3T MRI dataset and algorithm for prostate cancer detection. Computers in Biology and Medicine, 2022, 148, 105817. | 7.0 | 17 |
| 10 | Artificial intelligence to detect MYC translocation in slides of diffuse large B-cell lymphoma. Virchows Archiv Fur Pathologische Anatomie Und Physiologie Und Fur Klinische Medizin, 2021, 479, 617-621. | 2.8 | 14 |
| 11 | Artificial intelligence assistance significantly improves Gleason grading of prostate biopsies by pathologists. Modern Pathology, 2021, 34, 660-671. | 5.5 | 84 |
| 12 | Deep Learning Methods for Lung Cancer Segmentation in Whole-Slide Histopathology Images—The ACDC@LungHP Challenge 2019. IEEE Journal of Biomedical and Health Informatics, 2021, 25, 429-440. | 6.3 | 51 |
| 13 | Neural Image Compression for Gigapixel Histopathology Image Analysis. IEEE Transactions on Pattern Analysis and Machine Intelligence, 2021, 43, 567-578. | 13.9 | 125 |
| 14 | Mini Review: The Last Mile—Opportunities and Challenges for Machine Learning in Digital Toxicologic Pathology. Toxicologic Pathology, 2021, 49, 714-719. | 1.8 | 6 |
| 15 | End-to-end classification on basal-cell carcinoma histopathology whole-slides images. , 2021, , . | | 1 |
| 16 | Optimized tumour infiltrating lymphocyte assessment for triple negative breast cancer prognostics. Breast, 2021, 56, 78-87. | 2.2 | 18 |
| 17 | Deep learning in histopathology: the path to the clinic. Nature Medicine, 2021, 27, 775-784. | 30.7 | 355 |
| 18 | Residual cyclegan for robust domain transformation of histopathological tissue slides. Medical Image Analysis, 2021, 70, 102004. | 11.6 | 48 |

| # | Article | IF | CITATIONS |
|----|--|------|-----------|
| 19 | Artificial Intelligence for Diagnosis and Gleason Grading of Prostate Cancer in Biopsies—Current Status and Next Steps. European Urology Focus, 2021, 7, 687-691. | 3.1 | 18 |
| 20 | Detection of Prostate Cancer in Whole-Slide Images Through End-to-End Training With Image-Level Labels. IEEE Transactions on Medical Imaging, 2021, 40, 1817-1826. | 8.9 | 48 |
| 21 | Automated deep-learning system for Gleason grading of prostate cancer using biopsies: a diagnostic study. Lancet Oncology, The, 2020, 21, 233-241. | 10.7 | 407 |
| 22 | The 2019 International Society of Urological Pathology (ISUP) Consensus Conference on Grading of Prostatic Carcinoma. American Journal of Surgical Pathology, 2020, 44, e87-e99. | 3.7 | 292 |
| 23 | Impact of rescanning and normalization on convolutional neural network performance in multi-center, whole-slide classification of prostate cancer. Scientific Reports, 2020, 10, 14398. | 3.3 | 40 |
| 24 | Predicting MYC translocation in HE specimens of diffuse large B-cell lymphoma through deep learning. , 2020, , . | | 2 |
| 25 | Multi-class semantic cell segmentation and classification of aplasia in bone marrow histology images. , 2020, , . | | Ο |
| 26 | State-of-the-Art Deep Learning in Cardiovascular Image Analysis. JACC: Cardiovascular Imaging, 2019, 12, 1549-1565. | 5.3 | 238 |
| 27 | No pixel-level annotations needed. Nature Biomedical Engineering, 2019, 3, 855-856. | 22.5 | 14 |
| 28 | Quantifying the effects of data augmentation and stain color normalization in convolutional neural networks for computational pathology. Medical Image Analysis, 2019, 58, 101544. | 11.6 | 311 |
| 29 | Learning to detect lymphocytes in immunohistochemistry with deep learning. Medical Image Analysis, 2019, 58, 101547. | 11.6 | 98 |
| 30 | Epithelium segmentation using deep learning in H&E-stained prostate specimens with immunohistochemistry as reference standard. Scientific Reports, 2019, 9, 864. | 3.3 | 107 |
| 31 | Computer aided quantification of intratumoral stroma yields an independent prognosticator in rectal cancer. Cellular Oncology (Dordrecht), 2019, 42, 331-341. | 4.4 | 82 |
| 32 | A Single-Arm, Multicenter Validation Study of Prostate Cancer Localization and Aggressiveness With a Quantitative Multiparametric Magnetic Resonance Imaging Approach. Investigative Radiology, 2019, 54, 437-447. | 6.2 | 24 |
| 33 | From Detection of Individual Metastases to Classification of Lymph Node Status at the Patient Level: The CAMELYON17 Challenge. IEEE Transactions on Medical Imaging, 2019, 38, 550-560. | 8.9 | 269 |
| 34 | Robust and accurate quantification of biomarkers of immune cells in lung cancer micro-environment using deep convolutional neural networks. PeerJ, 2019, 7, e6335. | 2.0 | 24 |
| 35 | Lymph node detection in MR Lymphography: false positive reduction using multi-view convolutional neural networks. PeerJ, 2019, 7, e8052. | 2.0 | 12 |
| 36 | Resolution-agnostic tissue segmentation in whole-slide histopathology images with convolutional neural networks. PeerJ, 2019, 7, e8242. | 2.0 | 39 |

| # | Article | IF | CITATIONS |
|----|---|------|-----------|
| 37 | High resolution whole prostate biopsy classification using streaming stochastic gradient descent. , 2019, , . | | 0 |
| 38 | Machine Learning Compared With Pathologist Assessment—Reply. JAMA - Journal of the American Medical Association, 2018, 319, 1726. | 7.4 | 6 |
| 39 | Whole-Slide Mitosis Detection in H&E Breast Histology Using PHH3 as a Reference to Train Distilled Stain-Invariant Convolutional Networks. IEEE Transactions on Medical Imaging, 2018, 37, 2126-2136. | 8.9 | 184 |
| 40 | 1399 H&E-stained sentinel lymph node sections of breast cancer patients: the CAMELYON dataset. GigaScience, 2018, 7, . | 6.4 | 221 |
| 41 | Automated segmentation of epithelial tissue in prostatectomy slides using deep learning. , 2018, , . | | 11 |
| 42 | H&E stain augmentation improves generalization of convolutional networks for histopathological mitosis detection. , 2018, , . | | 14 |
| 43 | Automatic segmentation of histopathological slides of renal tissue using deep learning. , 2018, , . | | 23 |
| 44 | Automatic color unmixing of IHC stained whole slide images. , 2018, , . | | 7 |
| 45 | Using deep learning to segment breast and fibroglandular tissue in MRI volumes. Medical Physics, 2017, 44, 533-546. | 3.0 | 173 |
| 46 | A survey on deep learning in medical image analysis. Medical Image Analysis, 2017, 42, 60-88. | 11.6 | 7,976 |
| 47 | Diagnostic Assessment of Deep Learning Algorithms for Detection of Lymph Node Metastases in Women With Breast Cancer. JAMA - Journal of the American Medical Association, 2017, 318, 2199. | 7.4 | 2,003 |
| 48 | Comparison of different methods for tissue segmentation in histopathological whole-slide images. , 2017, , . | | 29 |
| 49 | Location Sensitive Deep Convolutional Neural Networks for Segmentation of White Matter Hyperintensities. Scientific Reports, 2017, 7, 5110. | 3.3 | 171 |
| 50 | The importance of stain normalization in colorectal tissue classification with convolutional networks. , 2017, , . | | 105 |
| 51 | Evaluation of tongue squamous cell carcinoma resection margins using ex-vivo MR. International Journal of Computer Assisted Radiology and Surgery, 2017, 12, 821-828. | 2.8 | 20 |
| 52 | Large scale deep learning for computer aided detection of mammographic lesions. Medical Image Analysis, 2017, 35, 303-312. | 11.6 | 728 |
| 53 | Context-aware stacked convolutional neural networks for classification of breast carcinomas in whole-slide histopathology images. Journal of Medical Imaging, 2017, 4, 1. | 1.5 | 126 |
| 54 | MAGE expression in head and neck squamous cell carcinoma primary tumors, lymph node metastases and respective recurrences-implications for immunotherapy. Oncotarget, 2017, 8, 14719-14735. | 1.8 | 21 |

GEERT JS LITJENS

| # | Article | IF | CITATIONS |
|----|---|------|-----------|
| 55 | Deep learning as a tool for increased accuracy and efficiency of histopathological diagnosis. Scientific Reports, 2016, 6, 26286. | 3.3 | 764 |
| 56 | Automated multistructure atlasâ€essisted detection of lymph nodes using pelvic MR lymphography in prostate cancer patients. Medical Physics, 2016, 43, 3132-3142. | 3.0 | 2 |
| 57 | Automated Detection of DCIS in Whole-Slide H&E Stained Breast Histopathology Images. IEEE Transactions on Medical Imaging, 2016, 35, 2141-2150. | 8.9 | 68 |
| 58 | In-depth tissue profiling using multiplexed immunohistochemical consecutive staining on single slide. Science Immunology, 2016, 1, aaf6925. | 11.9 | 142 |
| 59 | Pulmonary Nodule Detection in CT Images: False Positive Reduction Using Multi-View Convolutional Networks. IEEE Transactions on Medical Imaging, 2016, 35, 1160-1169. | 8.9 | 926 |
| 60 | Stain Specific Standardization of Whole-Slide Histopathological Images. IEEE Transactions on Medical Imaging, 2016, 35, 404-415. | 8.9 | 218 |
| 61 | Computer-extracted Features Can Distinguish Noncancerous Confounding Disease from Prostatic Adenocarcinoma at Multiparametric MR Imaging. Radiology, 2016, 278, 135-145. | 7.3 | 43 |
| 62 | Intranodal signal suppression in pelvic MR lymphography of prostate cancer patients: a quantitative comparison of ferumoxtran-10 and ferumoxytol. PeerJ, 2016, 4, e2471. | 2.0 | 8 |
| 63 | Multiparametric Magnetic Resonance Imaging for Discriminating Low-Grade From High-Grade Prostate Cancer. Investigative Radiology, 2015, 50, 490-497. | 6.2 | 63 |
| 64 | Automated detection of prostate cancer in digitized whole-slide images of H and E-stained biopsy specimens. , 2015, , . | | 7 |
| 65 | Prostate Cancer: The European Society of Urogenital Radiology Prostate Imaging Reporting and Data System Criteria for Predicting Extraprostatic Extension by Using 3-T Multiparametric MR Imaging. Radiology, 2015, 276, 479-489. | 7.3 | 53 |
| 66 | A multi-scale superpixel classification approach to the detection of regions of interest in whole slide histopathology images. Proceedings of SPIE, 2015, , . | 0.8 | 19 |
| 67 | Clinical evaluation of a computer-aided diagnosis system for determining cancer aggressiveness in prostate MRI. European Radiology, 2015, 25, 3187-3199. | 4.5 | 57 |
| 68 | Quantitative identification of magnetic resonance imaging features of prostate cancer response following laser ablation and radical prostatectomy. Journal of Medical Imaging, 2014, 1, 035001. | 1.5 | 11 |
| 69 | Distinguishing prostate cancer from benign confounders via a cascaded classifier on multi-parametric MRI. Proceedings of SPIE, 2014, , . | 0.8 | 11 |
| 70 | Evaluation of prostate segmentation algorithms for MRI: The PROMISE12 challenge. Medical Image Analysis, 2014, 18, 359-373. | 11.6 | 469 |
| 71 | Computer-Aided Detection of Prostate Cancer in MRI. IEEE Transactions on Medical Imaging, 2014, 33, 1083-1092. | 8.9 | 338 |
| 72 | Distinguishing benign confounding treatment changes from residual prostate cancer on MRI following laser ablation. Proceedings of SPIE, 2014, , . | 0.8 | 0 |

| # | Article | IF | CITATIONS |
|----|---|-----|-----------|
| 73 | Assessment of Prostate Cancer Aggressiveness Using Dynamic Contrast-enhanced Magnetic Resonance Imaging at 3 T. European Urology, 2013, 64, 448-455. | 1.9 | 152 |
| 74 | Differentiation of Prostatitis and Prostate Cancer by Using Diffusion-weighted MR Imaging and MR-guided Biopsy at 3 T. Radiology, 2013, 267, 164-172. | 7.3 | 105 |
| 75 | Automated computer-aided detection of prostate cancer in MR images: from a whole-organ to a zone-based approach. Proceedings of SPIE, 2012, , . | 0.8 | 12 |
| 76 | Interpatient Variation in Normal Peripheral Zone Apparent Diffusion Coefficient: Effect on the Prediction of Prostate Cancer Aggressiveness. Radiology, 2012, 265, 260-266. | 7.3 | 66 |
| 77 | A Pattern Recognition Approach to Zonal Segmentation of the Prostate on MRI. Lecture Notes in Computer Science, 2012, 15, 413-420. | 1.3 | 50 |
| 78 | Automated 3â€dimensional segmentation of pelvic lymph nodes in magnetic resonance images. Medical Physics, 2011, 38, 6178-6187. | 3.0 | 17 |
| 79 | Automatic computer aided detection of abnormalities in multi-parametric prostate MRI. Proceedings of SPIE, 2011, , . | 0.8 | 28 |
| 80 | Required Accuracy of MR-US Registration for Prostate Biopsies. Lecture Notes in Computer Science, 2011, , 92-99. | 1.3 | 2 |
| 81 | Pharmacokinetic models in clinical practice: What model to use for DCE-MRI of the breast?. , 2010, , . | | 7 |
| 82 | Simulation of Nodules and Diffuse Infiltrates in Chest Radiographs Using CT Templates. Lecture Notes in Computer Science, 2010, 13, 396-403. | 1.3 | 2 |
| 83 | Computer Aided Detection of Prostate Cancer Using T2, DWI and DCE MRI: Methods and Clinical Applications. Lecture Notes in Computer Science, 2010. , 4-14. | 1.3 | 1 |